BIOCHEMISTRY
including biophysical chemistry & molecular biology

Article

pubs.acs.org/biochemistry

Response of GWALP Transmembrane Peptides to Changes in the Tryptophan Anchor Positions

Vitaly V. Vostrikov* and Roger E. Koeppe, II

Department of Chemistry and Biochemistry, University of Arkansas, Fayetteville, Arkansas 72701, United States

Supporting Information

ABSTRACT: While the interfacial partitioning of charged or aromatic anchor residues may determine the preferred orientations of transmembrane peptide helices, the dependence of helix orientation on anchor residue position is not well understood. When anchor residue locations are changed systematically, some adaptations of the peptide–lipid interactions may be required to compensate for the altered interfacial interactions. Recently, we have developed a novel transmembrane peptide, termed GW^{5,19}ALP23 (acetyl-GGALW^{5}LALALALALALW^{19}LAGA-ethanolamide), which proves to be a well-behaved sequence for an orderly investigation of protein–lipid interactions. Its roughly symmetric nature allows for shifting the anchoring Trp residues by one Leu-Ala pair inward (GW^{7,17}ALP23) or outward (GW^{3,21}ALP23), thus providing fine adjustments of the formal distance between the tryptophan residues. With no other obvious anchoring features present, we postulate that the inter-Trp distance may be crucial for aspects of the peptide–lipid interaction. Importantly, the amino acid composition is identical for each of the resulting related GWALP23 sequences, and the radial separation between the pairs of Trp residues on each side of the transmembrane α-helix remains similar. Here we address the adaptation of the aforementioned peptides to the varying Trp locations by means of solid-state ^{2}H nuclear magnetic resonance experiments in varying lipid bilayer membrane environments. All of the GW^{x,y}ALP23 sequence isomers adopt transmembrane orientations in DOPC, DMPC, and DLPC environments, even when the Trp residues are quite closely spaced, in GW^{7,17}ALP23. Furthermore, the dynamics for each peptide isomer are less extensive than for peptides possessing additional interfacial Trp residues. The helical secondary structure is maintained more strongly within the Trp-flanked core region than outside of the Trp boundaries. Deuterium-labeled tryptophan indole rings in the GW^{x,y}ALP23 peptides provide additional insights into the behavior of the Trp side chains. A Trp side chain near the C-terminus adopts a different orientation and undergoes somewhat faster dynamics than a corresponding Trp side chain located an equivalent distance from the N-terminus. In contrast, as the inter-Trp distance changes, the variations among the average orientations of the Trp indole rings at either terminus are systematic yet fairly small. We conclude that subtle adjustments to the peptide tilt, and to the N- and C-terminal Trp side chain torsion angles, permit the GW^{x,y}ALP23 peptides to maintain preferred transmembrane orientations while adapting to lipid bilayers with differing hydrophobic thicknesses.

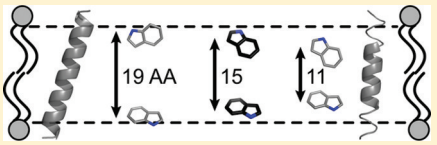

The influence of a lipid bilayer membrane on protein organization and function is well-documented. For example, the orientation (tilt) angles of virus protein "u"[1] and of the GABA$_A$ receptor[2] have been shown to vary in response to the thickness of the lipid bilayer. The lipid acyl chain identities furthermore influence the assembly of M2 tetramer proton channels[3] and alter the functional equilibrium of rhodopsin.[4]

Protein transmembrane domains and membrane protein function are governed in part by the interfacial or aqueous partitioning of aromatic or charged anchor residues that flank the transmembrane helical domains. These types of residues are enriched at the interfaces,[5,6] with the preferred position for lysines being ~3 Å farther from the bilayer center than the preferred positions for tryptophans.[7] To improve our understanding of the influence of interfacial anchoring residues, systematic approaches are quite helpful. It is in this regard useful to consider combinations of synthetic lipids and model peptides, which make it feasible to adjust systematically the distances between anchor residues and the thickness of the lipid matrix.[8−11] Such model peptide sequences typically have been based on a repeating sequence unit, wherein the addition or removal of an extra hydrophobic block will alter the length of the transmembrane domain with minimal disruption of other properties. For example, in "WALP" family peptides [GWW-(LA)$_n$LWWA],[9,12,13] the effective hydrophobic length of the core helix between the Trp residues changes as n is varied. In these peptides, the core helix is bounded by the aromatic side chains of Trp. With regard to the modulation of lipid-phase behavior, the effective length of a WALP peptide is governed by the distance between the innermost Trp residues that flank the core helix.[14] Furthermore, because Trp and also Tyr are particularly prevalent at the membrane–water interface in membrane proteins of known structure,[5,6,15] changing the placements of aromatic residues could offer a means of modifying the orientation and behavior of the membrane-spanning domain. Conversely, the lipid thickness can be varied by altering the acyl chain lengths, a factor that may compensate when anchor residue positions are changed. When acyl chains

Received: April 27, 2011
Revised: July 29, 2011
Published: August 1, 2011

longer than 14 carbons are utilized, nevertheless, one or more double bonds must be introduced (in some or all of the chains) to maintain appropriate lipid bilayer fluidity at physiological temperature.

Even such seemingly "simple" peptide–lipid systems may pose a number of issues. The lipid unsaturation will also influence the lipid lateral pressure profile.[16] For the peptide, in addition to the length of the core helix between the anchor residues, the identities of the polar, amphiphilic, and/or aromatic interfacial residues may alter the response of the system.[17] Furthermore, the geometry of a helix dictates that adding or removing core helix residues inevitably also will change the radial positions of the anchoring side chains.[18] A further potential issue concerns the overall hydrophobicity of the peptide system in cases where small "blocks" of sequence are added or removed. The sequences with smaller numbers of amino acids thereby may become too polar to insert into a lipid bilayer or too short to form stable helices,[19] which could lead to oligomerization.[20]

Recently, we improved the design of WALP family peptides by replacing two of the tryptophans with glycines.[21] Unexpectedly, the dependence of the WALP peptide apparent tilt angle on the lipid bilayer thickness is not straightforward. The relatively minor response of the original WALP peptides to changes in the lipid thickness was later explained in terms of extensive dynamics.[22,23] The dynamics can be rationalized in terms of an excess of interfacial tryptophan residues, dispersed around a helical wheel,[18] and potentially competing among themselves for favorable interactions with the headgroups of the lipids.[17,24]

To circumvent some of these limitations, we developed GW^{5,19}ALP23 (GGALW[LA]$_6$LWLAGA), which proves to be a well-behaved transmembrane peptide for the systematic investigation of protein–lipid interactions.[17,25] In this study, we further exploit its orderly sequence, which allows for shifting the remaining individual Trp residues either inward or outward in pairwise fashion, thereby leading to sequences of the form GW^{x,y}ALP23, where the *x,y* pairs designate the Trp sequence positions, either 5,19 (original GWALP23), 3,21 (Trp residues moved outward), or 7,17 (Trp residues moved inward). These sequences allow for fine-tuning the length of the core (Leu-Ala)$_n$ helix, while maintaining identical amino acid composition and therefore identical overall peptide hydrophobicity. Furthermore, because in each case one Trp of GWALP23 is moved radially by +200° and the other by −200°, they effectively "meet" on another face of the helix and thereby maintain a similar radial separation on one side of an α-helix in each of the three peptides (Table 1 and Figure 1). The Trp residues on both ends of GW^{x,y}ALP23 have a substantial propensity to reside at the lipid–water interface.[26,27] To maintain effective interactions, it is conceivable that the single indole rings at either end may alter their side chain orientations to adapt in different lipid environments.[28] For these reasons, we undertake a comprehensive solid-state NMR investigation of the generalized whole-peptide and specific indole-ring responses of GW^{x,y}ALP23 transmembrane peptides to varying lipid environments. We employ deuterated alanines to investigate the peptide helix average orientations and dynamics and deuterated tryptophans to investigate the indole side chain adjustments. The intent is to provide an enhanced understanding of how lipids influence the behavior of membrane-spanning peptides.

Table 1. Sequences of GW^{x,y}ALP23 Peptides[a]

Peptide	Sequence
GW^{3,21}ALP23	GG**W**LALALALALALALALAL**W**GA
GW^{5,19}ALP23	GGAL**W**LALALALALALAL**W**LAGA
GW^{7,17}ALP23	GGALAL**W**LALALALAL**W**LALAGA

[a]The N-terminal Gly residue is acetylated. The C-terminal Ala residue is blocked with ethanolamide.

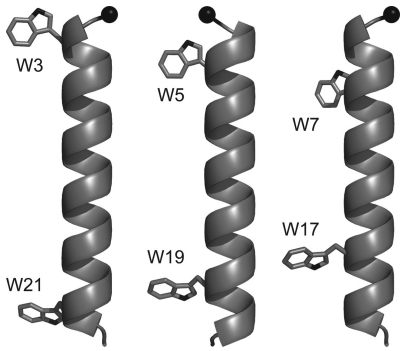

Figure 1. Molecular models of GW^{3,21}ALP, GW^{5,19}ALP23, and GW^{7,17}ALP23 (from left to right, respectively). The black sphere indicates the C$_\alpha$ of Gly1. Note that the GW^{5,19}ALP23 model is rotated by 180°.

MATERIALS AND METHODS

All isotope-enriched compounds were from Cambridge Isotope Laboratories (Andover, MA). Deuterium-labeled alanine (Ala-d_4) and tryptophan (Trp-d_5; deuterons on the indole ring) were modified by manual synthesis to introduce a fluorenylmethoxycarbonyl (Fmoc) group, using an identical protocol for both amino acids.[29] Partial hydrogen–deuterium exchange on the Trp indole side chain was accomplished by incubating commercial Fmoc-Trp (NovaBiochem, San Diego, CA) with deuterated trifluoroacetic acid (TFA-d_1) at 10 °C for 3 h.[30] This procedure facilitates incorporation of deuterium at positions 2 and 5 of the indole ring, which was confirmed by ^{1}H NMR spectroscopy in DMSO-d_6, by means of the intensity reduction at position 2 and changes in the multiplet pattern at positions 4 and 6 (Figure S1 of the Supporting Information). The peptides synthesized with TFA-d_1-treated Fmoc-Trp represent a mixture of GW^{x,y}ALP23-Trp-d_0, GW^{x,y}ALP23-Trp-d_1, and GW^{x,y}ALP23-Trp-d_2. For the sake of brevity, we further refer to them in the form of GW^{x,y}ALP23-Trp-d_2.

Peptides were synthesized utilizing a model 433A peptide synthesizer (Applied Biosystems by Life Technologies, Foster City, CA) in a manner similar to that for GWALP23,[17] using Wang resin and Fmoc-protected amino acids (NovaBiochem). Deuterium-enriched alanines were introduced in pairs at different isotope abundance levels. Deuterium-enriched tryptophans were incorporated in separate peptides one at a time; namely, for each GW^{x,y}ALP23 sequence, four separate Trp-labeled peptides were synthesized (having full or partial deuteration of the N- or C-terminal Trp). Because of the mild conditions for cleavage of the peptide from the Wang resin (20% ethanolamine in dichloromethane), no side chain protecting groups were required.[31] Peptides were purified by

dx.doi.org/10.1021/bi2006459 | Biochemistry 2011, 50, 7522–7535

reversed-phase HPLC (C8), using the previously established conditions for GWALP23.[17] Confirming HPLC chromatograms and mass spectra are provided in the Supporting Information (Figures S2 and S3).

Circular dichroism (CD) spectra were obtained for peptides incorporated into small unilamellar vesicles (1:40 peptide:lipid ratio) produced by an ultrasonic treatment. Peptide concentrations were determined spectrophotometrically to be in the 100 μM range. CD spectra were recorded using a 1 mm path length cell and a Jasco (Easton, MD) J710 spectropolarimeter operated at a scan rate of 20 nm/min and a bandwidth of 1.0 nm. Five spectra were averaged to enhance the signal intensities. Aliquots of the same samples were further diluted 50-fold for steady-state fluorescence spectroscopy, using a Perkin-Elmer LS-55 fluorescence spectrometer. The excitation wavelength was 284 nm, and emission was recorded between 300 and 500 nm at a rate of 200 nm/min. Slit widths were 7.5 nm, for both excitation and emission. An asymmetric cuvette was employed, having a 10 mm path length for excitation and a 1 mm path length for emission. Ten spectra were acquired and averaged.

Samples for solid-state ^{2}H NMR were prepared by mechanical alignment, as described previously.[12] A mixture of 2 μmol of peptide and 80 μmol of lipid (Avanti, Alabaster, AL) was deposited on glass slides (4.8 mm × 23 mm × 0.07 mm) from a methanol/water mixture (95:5), dried in vacuo (10^{-3} Torr), and hydrated with ^{2}H-depleted water to a 45% level of hydration (w/w). Glass slides were stacked and sealed in a glass cuvette (4.9 mm × 4.9 mm × 24 mm). Deuterium NMR spectra were recorded using two Bruker (Billerica, MA) Avance 300 spectrometers operating at a magnetic field of 7.0 T, utilizing probes with a cylindrical 8 mm coil and a quadrupolar echo pulse sequence with full phase cycling.[32] The spectral width was 1 MHz, with a recycle delay of 90 ms and pulse durations of 3.2 or 4.5 μs (depending on the spectrometer probe). Approximately 700000 transients were collected for Ala-d_4 peptides and twice that number for Trp-d_x peptides. Spectra for Ala-labeled peptides were processed by zero filling the time domain to 5120 points, applying 100 Hz exponential apodization and Fourier transformation. The corresponding parameters for the spectra of Trp-labeled peptides were 2048 data points and 300 Hz. Spectra were recorded at two sample orientations, with the lipid bilayer normal either parallel (β = 0°) or perpendicular (β = 90°) to the applied magnetic field. An average value of the quadrupolar splitting magnitude was taken (after applying the scaling factor of 2 for the β = 90° orientation), the standard deviation between the two sample orientations typically being within 0.5 kHz.

Geometric analysis of labeled alanines (GALA)[12] was performed by fitting a generalized order parameter S_{zz}, and the apparent peptide tilt magnitude (τ) and direction (ρ), to a model of a tilted α-helical peptide, with an $\varepsilon_\parallel$ angle between the alanine C_α−C_β bond vector and peptide helix axis equal to 59.4°.[12] Further, we refer to this S_{zz} value as S_{pept} to avoid confusion with the tryptophan side chain order parameter (see below). Selected peptide−lipid systems were analyzed also by considering Gaussian distributions of tilt and rotation around the average values (τ_0 and ρ_0, respectively) with standard deviations (σ_τ and σ_ρ, respectively).[22] In these cases, the order parameter was fixed at 0.88 and a multidimensional grid search was performed by varying σ_ρ between 0° and 200°, σ_τ between 0° and 30°, τ_0 between 0° and 90°, and ρ_0 between 0° and 359°, using 1° increments.

Deuterium NMR data from Trp-labeled peptides were analyzed by rotating the previously refined structure of 3-methylindole[33] by two angles, ρ_1 and ρ_2 (defined in Figure S4 of the Supporting Information), and considering the dynamics in the form of an order parameter, S_{zz},[30,34] which now would incorporate side chain as well as backbone dynamics. Because of symmetry considerations, such analysis returns eight possible orientations of the indole ring; we report the values for one unique octet defined by $0° \le \rho_1 \le 180°$ and $0° \le \rho_2 \le 90°$ (Figure S4 of the Supporting Information). While the fully deuterated Trp side chain has five deuterons, the C−D bond vectors at carbons 4 and 7 are nearly collinear (angle of 179.3°[33]) and therefore are generally not resolved.

Indeed, it was assumed that deuterons at positions 4 and 7 are not distinguishable and produce identical signals, because none of the Trp-d_5 spectra had five resolved peaks. Because the spectral assignments are not known, initially 4! = 24 possible assignment schemes were considered for each Trp. (The number was later reduced in systems for which Trp-d_2 data were available.) For estimating the root-mean-square deviation (rmsd), we treat positions 4 and 7 separately, under the assumption that the corresponding NMR signal represents a superposition of these deuterons. Assignment schemes were selected on the basis of the S_{zz} and rmsd values, as explained in Results.

For the conversion of backbone-independent (ρ_1 and ρ_2) angles to Trp side chain (χ_1 and χ_2) angles, models of GW^{x,y}ALP23 were constructed using Swiss-PdbViewer 4.0[35] using (Φ, Ψ, Ω) of (−65°, −40°, 180°) and rotated by angles τ and ρ according to Table 3 (see Results) to yield the coordinates of the tilted peptides. The side chain of a tryptophan residue in question was rotated around the χ_1 and χ_2 angles to yield the indole orientation matching the previously obtained ρ_1 and ρ_2 angles of 3-methylindole. Steric hindrance contours were generated by rotating the Trp side chains through the complete range of χ_1 and χ_2 angles. Steric clash was defined as the distance of <2 Å between any of the non-hydrogen atoms of the indole ring and any non-hydrogen atoms of the peptide backbone.

RESULTS

Both leucine and alanine are considered to have strong α-helix propensity, while tryptophan does not exhibit this property.[36] A lipid bilayer typically offers a stabilizing environment for the transmembrane helices, because it is favorable to maximize the backbone hydrogen bonding in the nonpolar lipid environment.[37] Nevertheless, in the case of a lipid with short acyl chains (DLPC), several residues at the peptide termini may protrude into the interfacial and/or aqueous phases, where deviations from the helical structure can occur more easily. To assess the secondary structure of the GW^{x,y}ALP23 peptides, we have recorded CD spectra of the peptides in DLPC (Figure 2).

All three GW^{x,y}ALP23 peptides exhibit the spectral signature of an α-helix, with a distinct minimum at 208 nm and a broad shoulder around 222 nm. Nevertheless, the mean residue ellipticity values for GW^{7,17}ALP23 are somewhat lower (~15% reduced in magnitude) in comparison with those of the other peptides, suggesting a reduced level of helical structure when the tryptophans are moved inward. It is widely accepted that due to their amphiphilic character the tryptophan residues

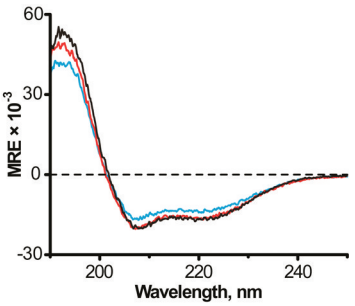

Figure 2. Circular dichroism spectra of $GW^{3,21}$ALP23 (black), $GW^{5,19}$ALP23 (red), and $GW^{7,17}$ALP23 (blue) in DLPC.

prefer the membrane−water interface, which would position the terminal residues 1−6 and 18−23 of $GW^{7,17}$ALP23 in more polar regions, where some helix unwinding may be expected.[38] The spectral intensities of $GW^{5,19}$ALP23 and $GW^{3,21}$ALP23 overlap, indicative of similar helicity. Previously, we have observed some fraying of the $GW^{5,19}$ALP23 termini in DMPC;[17] within this context, the CD data suggest that the $GW^{3,21}$ALP23 helix could possibly terminate prior to the Trp residues in DLPC.

Earlier studies with the peptides of the WALP family demonstrated a peptide length-dependent formation of non-bilayer phases of phosphatidylcholine membranes at high peptide:lipid ratios: in the case of negative hydrophobic mismatch, the lipid phase can undergo transitions from lamellar to isotropic to inverse hexagonal phase.[9] To probe this possibility for $GW^{x,y}$ALP23 peptides, phosphorus NMR spectra of oriented samples were recorded. For all of the peptide−lipid combinations under investigation here, using a molar ratio of 1:40 (peptide:lipid), the ^{31}P NMR spectra were characteristic of bilayer lipids, with a chemical shift anisotropy of ∼42 ppm (Figure S5 of the Supporting Information).

To gain insight into the behavior of $GW^{x,y}$ALP23 peptides in lipid bilayer membranes of varying thickness, we introduced deuterium-labeled Ala residues into the core helical sequence between the tryptophans. Previously, we have observed that $GW^{5,19}$ALP23 readily incorporates into lipid bilayers composed of C12−C18 lipids, remains helical, and adopts well-defined average orientations that vary with lipid thickness.[17,21] We find similar responses when the tryptophans are moved inward or outward to effectively decrease or increase the length of the Leu-Ala core sequence between the tryptophans (Figure 3). The Ala methyl ^{2}H quadrupolar splittings ($\Delta\nu_q$) of these peptides are dependent on the macroscopic sample orientation, indicating fast precession of each helix about the lipid bilayer normal.[39] A full set of ^{2}H NMR spectra is provided in Figures S6−S8 of the Supporting Information, and the $\Delta\nu_q$ magnitudes are listed in Table 2. For the spectra in Figure 3 and Figures S6−S8 of the Supporting Information, the peptide:lipid molar ratio is 1:40; nevertheless, the $\Delta\nu_q$ magnitudes change very little when the ratio is reduced to 1:200 (Figure S9 of the Supporting Information). The quadrupolar splittings of centrally positioned alanine residues change from 20.9 to 23.2 kHz (A11) and from 3.8 to 9.6 kHz (A13) as the peptide:lipid ratio is decreased 5-fold, from 1:40 to 1:200. Because the magnitude of quadrupolar splittings is described by eq 1, the $\Delta\nu_q$ values relate to changes in θ, the angle between a particular alanine $C_\alpha-C_\beta$ bond vector and the

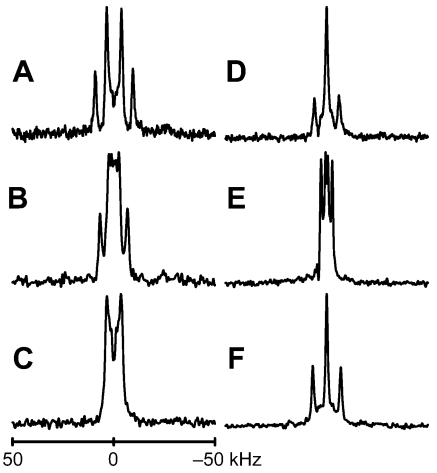

Figure 3. Deuterium NMR spectra of peptides in DMPC: (A−D) $GW^{3,21}$ALP23 and (E and F) $GW^{7,17}$ALP23. Labeled positions are 5 and 7 (A), 9 and 11 (B and E), 13 and 15 (C and F), and 17 and 19 (D). The sample orientation is $\beta = 0°$. A complete set of deuterium NMR spectra is provided in Figures S6−S8 of the Supporting Information.

applied magnetic field.

$$\Delta\nu_q = QCC \times S_{pept} \times \left[\frac{1}{2}(3\cos^2\theta - 1)\right]\left[\frac{1}{2}(3\cos^2\beta - 1)\right] \times \left\langle\frac{1}{2}(3\cos^2\gamma - 1)\right\rangle \quad (1)$$

Substitution of QCC = 168 kHz, S_{pept} = 0.88 (Table 3), $\beta = 0°$, and $\gamma = 109.5°$ (the tetrahedral angle to account for the methyl group rotation) leads to the angle θ (for the average peptide orientation) changing from 43.8° to 42.6° for A11 and from 52.7° to 49.6° for A13. From eq 1, it follows that the closer θ is to the magic angle (∼54.7°), the more sensitive $\Delta\nu_q$ become to even minor deviations of θ [note the steep slope of the helical wave in the vicinity of A13 (Figure 4B)]. The small changes in the θ angles when the peptide:lipid ratio is diluted from 1:40 to 1:200 are in accord with the earlier finding of only a shallow dependence of $\Delta\nu_q$ or θ on the ratio of $GW^{5,19}$ALP23 to DMPC being between 1:40 and 1:80.[17] These results furthermore illustrate that the ^{2}H $\Delta\nu_q$ values are very sensitive to small changes in the Ala residue orientations.

From the dependence of $\Delta\nu_q$ on the Ala residue position, it is apparent that each of the peptides is tilted to a preferred average orientation in the lipid bilayer membranes. It is notable that the peptide with only nine amino acids between the Trp residues ($GW^{7,17}$ALP23) maintains a preferred, nonrandom, transmembrane orientation, not only in the thinner membranes but also in DOPC. While the membrane incorporation is not overly surprising, because of the overall hydrophobicity,[40] the rather consistent helix orientation (on average) nevertheless contrasts with that of several peptides and peptaibols (which lack Trp residues), which switch from a transmembrane to an interfacially bound topology as a function of lipid bilayer thickness.[41−43] Even for $GW^{7,17}$ALP23 in DOPC, the tryptophans still seem to be important and significant for determining the average orientation and dynamics of the core helix.

dx.doi.org/10.1021/bi2006459 | Biochemistry 2011, 50, 7522−7535

Table 2. Alanine $C_\beta D_3$ Quadrupolar Splittings for GW^{x,y}ALP23 Peptides Incorporated into Lipid Bilayers[a]

		alanine position							
peptide	lipid	5	7	9	11	13	15	17	19
GW^{7,17}ALP23	DLPC	8.0	–	6.1	6.1	12.5	0.8	–	7.4
	DMPC	10.9	–	11.2	2.1	13.9	0.8	–	4.1
	DOPC	12.5	–	10.9	3.1	13.4	0.8	–	3.0
GW^{5,19}ALP23[b]	DLPC	–	26.4	25.5	26.9	14.6	20.7	3.4	–
	DMPC	–	21.9	8.9	20.9	3.8	17.6	2.9	–
	DOPC	–	16.6	1.7	16.7	1.5	15.4	2.6	–
GW^{3,21}ALP23	DLPC	19.6	23.8	15.7	18.7	0.9	9.6	11.4	0.8
	DMPC	6.4	17.9	5.2	13.6	6.7	6.7	12.2	0.8
	DOPC	0.8	13.1	2.1	9.3	6.6	6.6	12.3	1.3

[a]Values in kilohertz. Entries left blank were not measured because Trp is present instead of Ala. [b]Data from ref 17.

Table 3. GALA Fit Results for GW^{x,y}ALP23 Peptides in Lipid Bilayer Membranes[a]

peptide	S_{pept}	τ (deg)	ρ (deg)	rmsd (kHz)
DLPC				
GW^{7,17}ALP23	0.79	6.7	223	0.1
GW^{5,19}ALP23[a]	0.71	20.8	304	0.7
GW^{3,21}ALP23[b]	0.63	18.0	281	2.0
DMPC				
GW^{7,17}ALP23	0.82	4.3	182	0.1
GW^{5,19}ALP23[a]	0.88	9.1	310	1.1
GW^{3,21}ALP23	0.75	9.0	268	1.1
DOPC				
GW^{7,17}ALP23	0.83	4.0	186	0.1
GW^{5,19}ALP23[a]	0.86	6.1	322	0.6
GW^{3,21}ALP23	0.80	4.3	257	0.8

[a]Data for GW^{5,19}ALP23 from ref 17. [b]The rmsd for GW^{3,21}ALP23 in DLPC is reduced to 1.0 kHz if the A19 data point is omitted or to 1.5 kHz if the A5 data point is omitted. The corresponding S_{pept}, τ, and ρ values are 0.60, 19.7, and 277, respectively, with A19 omitted or 0.68, 15.3, and 283, respectively, with A5 omitted. Exclusion of both A5 and A19 leads to an rmsd of 0.9 kHz, with the corresponding parameters being 0.63, 18.0, and 279, respectively.

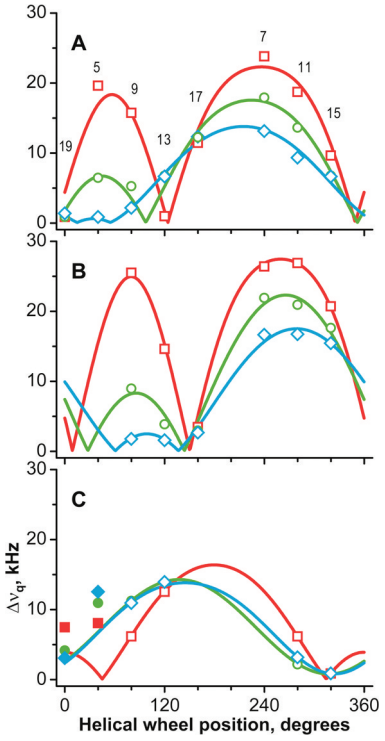

Figure 4. GALA helical wave plots of peptides in DLPC (red squares), DMPC (green circles), and DOPC (blue diamonds): (A) GW^{3,21}ALP23, (B) GW^{5,19}ALP23, and (C) GW^{7,17}ALP23. Deuterium-labeled alanine positions are denoted in panel A. Filled symbols correspond to residues outside the inter-Trp core not used for the analysis of helix orientation.

To determine the preferred molecular orientations, the deuterium NMR $\Delta\nu_q$ magnitudes for the GW^{x,y}ALP23 series peptides were subjected to GALA analysis, using implicit rigid-body dynamics in the form of a principal order parameter (S_{pept}) and peptide average orientation, namely, magnitude (τ_0) and direction (ρ_0), of the helix tilt as independent variables.[12] The fit quality was assessed by means of the rmsd between the observed and back-calculated $\Delta\nu_q$ values. A fit is typically considered good when the rmsd value is less than the ^{2}H peak line width (usually on the order of 1 kHz). It can be seen in Table 3 that this condition is fulfilled for each peptide–lipid system, with an exception of GW^{3,21}ALP23 in DLPC, where the rmsd approaches 2 kHz. This situation can be understood in terms of partial helix unwinding, as mentioned above. Even though the CD spectra were recorded from samples of sonicated vesicles, for which relatively high curvature is expected, the NMR spectra were recorded from oriented bilayer samples; the deductions about the extent of helicity, or partial fraying, show substantial agreement between the distributions of the alanine $\Delta\nu_q$ values and the observed CD spectra. We note, nevertheless, that the amount of helix unraveling at the peptide termini may be different between the vesicles and the aligned bilayers, as the solid-state NMR observables do not allow for expression of the extent of fraying quantitatively. Furthermore, the isotope labels were incorporated two residues away from an anchoring Trp residue, leaving open the possibility that helix unwinding could begin prior to the labeled alanines. Despite these caveats, the qualitatively similar results from the vesicle and oriented bilayer systems suggest that helix formation does not couple strongly with the bilayer curvature. Indeed, the exclusion of the most N-terminal data point (A5) of GW^{3,21}ALP23 in DLPC reduces the rmsd for the GALA fit to 1.5 kHz, while the exclusion of (only) the most C-terminal point (A19) leads to an rmsd of 1.0 kHz (Table 3). Conversely, excluding any individual central data point from A7 to A17 does not improve the fit quality, as the rmsd remains high, in the 1.9–2.1 kHz range when the data for A5 and A19 are present. Interestingly, introducing Arg12 or Arg14 into the GW^{3,21}ALP23 sequence leads to a large tilt and a

dx.doi.org/10.1021/bi2006459|Biochemistry 2011, 50, 7522–7535

good fit for the entire helix in DLPC.[44] When the $\Delta\nu_q$ value for A19 is excluded, the average orientation and dynamics of GW^{3,21}ALP23 in DLPC do not differ significantly from those obtained using all data points.

Earlier, we established, using ^{2}H labels for alanines 3 and 21, that the peptide helicity is not completely retained outside of the Trp-flanked core in GW^{5,19}ALP23.[17] While helix fraying near the water-exposed termini can be expected, the question of where the helix distortion begins to occur remains to be answered. To explore this question, we introduced Ala-d_4 at positions 5 and 19 in GW^{7,17}ALP23. These amino acids are located outside the two Trp residues yet still can be expected to be more buried than A3 and A21. Additionally, both A5 and A19 are capable of participating in a more extensive hydrogen bonding network because of the presence of a full complement of $i \pm 4$ residues. The $\Delta\nu_q$ values for alanines 5 and 19 in GW^{7,17}ALP23 are depicted with filled symbols in Figure 4C. The signals from A5 in each lipid differ by 5−10 kHz from theoretical values, calculated for a central (Leu-Ala)$_{4.5}$ helix of GW^{7,17}ALP23. On the other hand, the values for A19 appear quite close to the predicted values for the core helix in DMPC and DOPC, but not in DLPC. The results suggest that A5 is not helical in GW^{7,17}ALP23, whereas it appears that A19 does remain helical in thicker lipids but not in the thinner DLPC. The N-terminal segment appears to be more sensitive to helix unwinding, perhaps to accommodate an interfacial location for W7 in each of the lipid bilayer environments.

As a way of visualizing the quality of the GALA analyses, theoretical quadrupolar splittings were calculated and plotted as helical wave plots along with the observed $\Delta\nu_q$ magnitudes. Several points of interest emerge from examination of the GALA fits (Table 3 and Figure 4). The apparent tilt angles of the peptides fall within a relatively small range of ∼4−20°, in contrast to the rather large ranges of inter-tryptophan distances and lipid bilayer thicknesses used in the experiments (Table 4).

Table 4. Comparison of Trp Residue Spacing in GW^{x,y}ALP23 Peptides with Lipid Bilayer Membrane Hydrophobic Thickness[a]

	hydrophobic thickness	inter-Trp distance		
		GW^{3,21}ALP23	GW^{5,19}ALP23	GW^{7,17}ALP23
		27.0	21.0	15.0
			difference	
DLPC	19.5	+7.5	+1.5	−4.5
DMPC	23.0	+4.0	−2.0	−8.0
DOPC	27.0	0.0	−6.0	−12.0

[a]Distances are in angstroms. The inter-Trp distances are based on an increment of 1.5 Å per residue in a standard α-helix. The lipid bilayer hydrophobic thicknesses (from ref 59) do not include the headgroup regions.

We note for the respective peptide−lipid combinations that the difference between the inter-Trp distance and the bilayer hydrophobic thickness (not including the headgroups) spans a range of ∼20 Å (from −12 to 8 Å) (see Table 4). The average orientations and their uncertainties can also be examined on rmsd contour plots, constructed as a function of the τ and ρ angles (Figure 5). The trend in tilt angle magnitudes (τ) is not strictly linear; it appears instead that the tilt magnitudes reach limiting minimum and maximum values. Thus, GW^{7,17}ALP23 with the innermost Trp residues tilts by only ∼4−6° in each of the lipids, probably so that the Trp residues can approach as

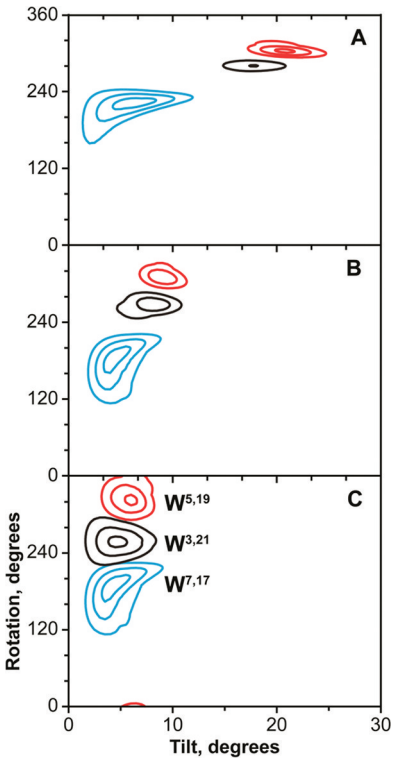

Figure 5. rmsd contour plots of GW^{3,21}ALP23 (black), GW^{5,19}ALP23 (red), and GW^{7,17}ALP23 (blue) in lipids: (A) DLPC, (B) DMPC, and (C) DOPC. Contour levels are plotted every 1 kHz; outer contour corresponds to 3 kHz.

closely as possible the bilayer interface while still maintaining the favorable entropy of the peptide precession about the bilayer normal.[45] Interestingly, both GW^{5,19}ALP23 and GW^{3,21}ALP23 have 18−21° apparent tilt values in DLPC. While dynamic averaging, beyond what can be treated in the analysis here using the available $|\Delta\nu_q|$ values, may increase the deduced apparent tilt by ∼10°,[22,46,47] it is nevertheless of interest that an apparent upper limit is reached with these neutral peptides. In terms of peptide dynamics, GW^{3,21}ALP23 exhibits a tendency toward lower S_{pept} values, suggestive of larger-amplitude motions when the Trp residues flank the long (Leu-Ala)$_{8.5}$ core sequence. As a general trend, the more widely spaced Trp residues in the environment of the shorter lipids tend to favor more extensive motions than vice versa.

Tryptophans reside preferentially in the interfacial region.[27,48,49] The region, nevertheless, does not have well-defined borders and spans quite a few angstroms.[50] Tryptophan intrinsic fluorescence is a well-known metric of the polarity of the medium in the immediate vicinity of the Trp indole ring, for which more hydrophobic environments shift the emission maximum (λ_{em}) to lower wavelengths (blue shifts).[51] This property of Trp has been used extensively to probe the hydrophobicity of its immediate environment.[11] The GW^{x,y}ALP23 sequences have one Trp residue on each side of the core α-helix; therefore, steady-state fluorescence may report the average polarity at the peptide termini (subject to considerations of the quantum yield). Despite the potential limitation of averaging over two indoles, the λ_{em} values of GW^{x,y}ALP23 peptides in different lipids show good correlation with the difference between the lipid thickness and Trp spacing along the α-helix (Figure 6). The observed λ_{em} values span a range of

dx.doi.org/10.1021/bi2006459|Biochemistry 2011, 50, 7522−7535

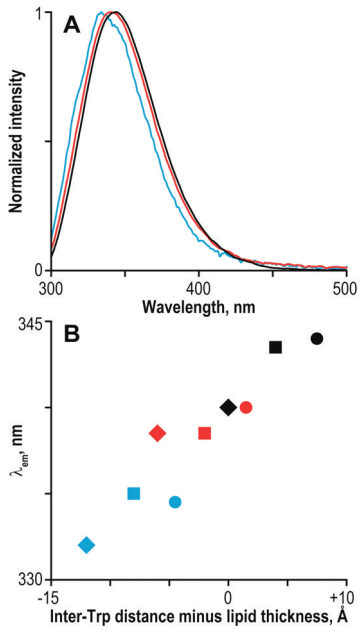

Figure 6. Steady-state fluorescence of GW^{x,y}ALP23 peptides. (A) Emission spectra of GW^{3,21}ALP23 (black), GW^{5,19}ALP23 (red), and GW^{7,17}ALP23 (blue) in DLPC small unilamellar vesicles. (B) Tryptophan emission maxima as a function of the difference between the inter-Trp distance and the lipid bilayer thickness (numerical values in Table 4). Peptides were GW^{3,21}ALP23 (black), GW^{5,19}ALP23 (red), and GW^{7,17}ALP23 (blue); lipids were DLPC (circles), DMPC (squares), and DOPC (diamonds).

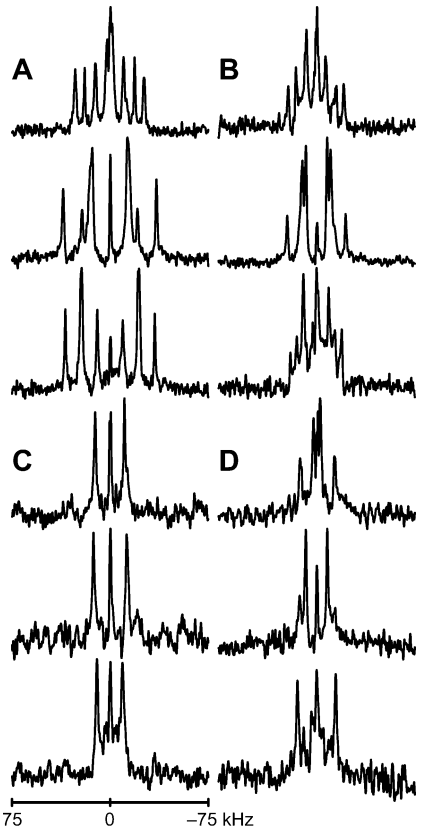

Figure 7. Deuterium NMR spectra of GW^{5,19}ALP23 labeled at the Trp side chain in DLPC, DMPC, and DOPC (from top to bottom, respectively): (A) N-terminal Trp5, full deuteration; (B) C-terminal Trp19, full deuteration; (C) N-terminal Trp5, partial deuteration; and (D) C-terminal Trp19, partial deuteration. Sample orientation $\beta = 90°$.

332−344 nm, indicative of an environment of graded polarity that is intermediate between those of the aqueous phase and the hydrophobic core of the lipid bilayer, as expected for the interfacial region.

The fluorescence spectra indicate that the average polarity of the environment around the indole rings changes as a function of the difference between the Trp spacing and the bilayer thickness. This observation raises questions of how peptide tilting could affect the orientations of the Trp side chains. One may speculate that reorientation of the helix axis may alter the indole ring spatial orientations. Alternatively, the Trp side chains may have restricted sets of orientations such that preferential positioning of the Trp indole rings could restrict the peptide tilt. To probe these questions, we have synthesized GW^{x,y}ALP23 peptides with deuterium labels on the indole rings and have recorded solid-state ^{2}H NMR spectra in different lipid bilayer membranes. Deuterium NMR spectra of partially (d_2) and fully (d_5) labeled indole rings of Trp residues of GW^{5,19}ALP23 are shown in Figure 7. A complete set of spectra for the fully labeled Trp residues in GW^{3,21}ALP23 and GW^{7,17}ALP23 is included in Figure S10 of the Supporting Information, and spectra of selected partially labeled Trp residues are shown in Figure S11 of the Supporting Information. Similar to earlier observations for WALP peptides,[28] larger quadrupolar splittings are observed for Trp residues that are near the N-terminus. Indeed, the largest $\Delta\nu_q$ value observed among the N-terminal Trp residues of the GW^{x,y}ALP23 peptides is 154 kHz, while the corresponding value for the set of C-terminal Trp residues is only 89 kHz. Alongside the signals from the ^{2}H-labeled Trp residues, the large number of scans sometimes led to background signals from the lipids and residual HDO.[25]

Typically, three or four resonances were observed for the d_5 indole ring and one or two for the partially labeled d_2 ring. Quadrupolar splitting magnitudes at $\beta = 0°$ and $\beta = 90°$ sample orientations were related by a factor of $^1/_2$, which is expected when there is rapid whole-molecule rotational averaging about the bilayer normal. Nevertheless, large contingents of sometimes quite weak resonances made it hard to observe many of the signals in the $\beta = 0°$ orientation. For this reason, the reported data are derived from the spectra of the samples in the $\beta = 90°$ orientation. The values observed in the $\beta = 90°$ orientation were then multiplied by a factor of 2 to simulate the expected values for the $\beta = 0°$ orientation (Table 5). Partially labeled samples often allowed the assignment of signals arising from the deuteron attached to indole carbon 2 and sometimes carbon 5. The assignments of these known signals were propagated to other samples where possible, using the least change principle. The remaining resonances were matched by fitting different assignment permutations to a model for the rotated indole ring and eliminating assignment schemes that led to high values of rmsd or unrealistic order parameters. The order parameter reflects the overall motion experienced by a system; in the case of Trp, therefore, it is feasible to deconvolute S_{zz} into terms for peptide S_{pept} and side chain S_{sc} motion, such that $S_{zz} = S_{pept}S_{sc}$ and $S_i \in [0,1]$. As reported above, the dynamics of GW^{x,y}ALP23 peptides encompass a range of 0.6−0.9 for S_{pept} (Table 3). This range establishes upper limits for the indole ring S_{zz}. Conversely, the side chain dynamics within the interfacial region are likely to be restricted

dx.doi.org/10.1021/bi2006459 | *Biochemistry* 2011, 50, 7522−7535

Table 5. Tryptophan Side Chain CD Quadrupolar Splitting Magnitudes for GW^{x,y}ALP23 Peptides Incorporated in Lipid Bilayer Membranes[a]

		$\Delta\nu_q$ (kHz) (for specific indole ring positions)							
		N-terminal Trp				C-terminal Trp			
peptide	lipid	(2)	(4/7)	(5)	(6)	(2)	(4/7)	(5)	(6)
GW^{7,17}ALP23	DLPC	67	63	154	74	54	63[d]	4	63[d]
	DMPC	54[b]	81	154	85	49[a]	67[d]	6[b]	67[d]
	DOPC	42[c]	77[c]			55	67[d]	8	67[d]
GW^{5,19}ALP23	DLPC	43[b]	8	105	76	61[a]	30	6[b]	85
	DMPC	54[b]	58	142	85	54[a]	43	33[b]	89
	DOPC	39[b]	86	137[b]	88	58[b]	39	8	78
GW^{3,21}ALP23	DLPC	64[b]	120	51[b]	15	53[b]	36	4	58
	DMPC	64[c]	145[c]	50[b,c]	42[c]	40[b,c]	27[c]		59[c]
	DOPC	62[c]	141[c]	52[b,c]		27[b,c]	19[c]	7[c]	51[c]

[a]Values were obtained from the $\beta = 90°$ sample orientation and were multiplied by 2. Entries left blank were not observed. [b]Value also observed in a partially deuterated sample. [c]Quadrupolar splittings have not been assigned to individual sites. [d]Signals not resolved.

because of steric hindrance. The value of S_{sc} is therefore likely to be quite high, which would place a lower limit on the overall Trp S_{zz} value.

Figure 8 shows rmsd as a function of S_{zz} for GW^{5,19}ALP23. Typically, for each peptide, a unique minimum was observed in such a plot for the N-terminal Trp, largely because of the high magnitude of $\Delta\nu_q$ at carbon 5, which could not be fitted by lower values of S_{zz}. The smaller range of quadrupolar splittings exhibited by the C-terminal tryptophans makes it possible to fit alternative ring orientations, manifest by several minima in the plots of rmsd versus S_{zz}. Nevertheless, in some cases, such as W19 in DMPC (Figure 8B), or W17 in all three lipids, only one global minimum was observed, with an S_{zz} value close to that observed also for the N-terminal Trp in the same peptide. On the basis of this finding, when a C-terminal Trp had multiple minima, we considered the one closest to the corresponding N-terminal Trp to be the global minimum, even if alternative fits might yield a slightly lower rmsd (Table 6). The uncertainties of the ρ_1 and ρ_2 angles at the S_{zz} global minimum can be visualized in a fashion similar to that for the peptide average orientation, using rmsd contour plots (Figure 9). It can be seen that the orientations of the N- and C-terminal Trp residues are distinct and differ primarily in the ρ_2 angle.

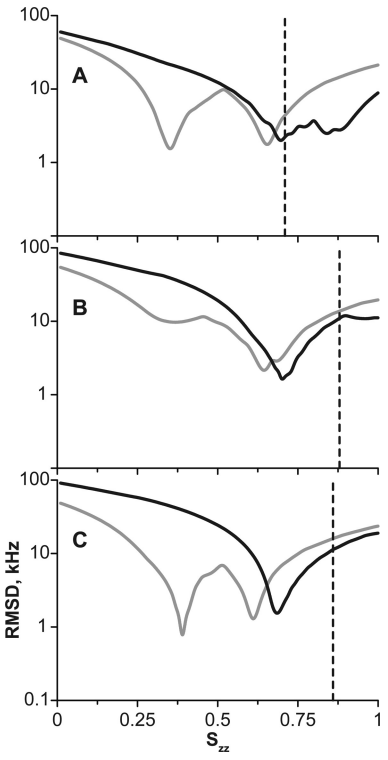

Figure 8. rmsd of fitting the N-terminal (black) and C-terminal (gray) tryptophans of GW^{5,19}ALP23 to the rotated indole model (note the logarithmic scale): (A) DLPC, (B) DMPC, and (C) DOPC. Angles ρ_1 and ρ_2 were optimized at each S_{zz} value to achieve the lowest possible rmsd. Each dashed line indicates the order parameter of the peptide (Table 3) and corresponds to the maximum possible value of the Trp S_{zz}.

In the case of W17 in GW^{7,17}ALP23, only three pairs of resonances can be identified in the spectra (Figure S10 of the Supporting Information). As the $\Delta\nu_q$ range for the C-terminal tryptophan residues is fairly small, it is conceivable that the missing signal is present, but not resolved because of spectral overlap. To account for this possibility, in each of the lipids we performed three separate fits of the W17 data by entering one of the quadrupolar splittings twice. Solutions were rejected on the basis of the previously described principles; in addition, the best fits among the different lipids were compared, as the C-terminal Trp in GW^{5,19}ALP23 has shown little variation in different bilayer membranes. A possible assignment with the intermediate $\Delta\nu_q$ value involving overlap of deuterons 4/7 and 2 was discarded because of the very different ρ_1 and ρ_2 angles (~70° and ~30°, respectively), in comparison with those of W19. Conversely, the conditions were readily fulfilled if the outermost quadrupolar splitting resulted from an overlap between deuterons at positions 4/7 and 6, which led to similar orientation angles and S_{zz} values for W17 and W19. Furthermore, in the ^{2}H NMR spectra of W17, the outermost signals typically were strongest. While the intensity alone is problematic to interpret in deuterium NMR spectroscopy (due to a number of factors, including radiofrequency power profile, contributions from powder pattern, etc.), the consideration of peak intensity nevertheless provides a valuable clue in combination with other factors. N-Terminal W7 produced four signals in DLPC and DMPC, allowing the assignments, but only two resolved resonances in DOPC, which did not provide sufficient restraints for the analysis.

dx.doi.org/10.1021/bi2006459 | Biochemistry 2011, 50, 7522–7535

Table 6. Tryptophan Side Chain Free Rotation Fit Values for GW^{x,y}ALP23 Peptides Incorporated in DLPC, DMPC, or DOPC[a]

		fit parameters[b]							
		N-terminal Trp				C-terminal Trp			
peptide	lipid	S_{zz}	ρ_1	ρ_2	rmsd	S_{zz}	ρ_1	ρ_2	rmsd
GW^{7,17}ALP23	DLPC	0.68	137	0	2.8	0.54	165	36	0.3
	DMPC	0.72	140	0	2.2	0.55	162	40	0.3
	DOPC					0.57	165	36	1.7
GW^{5,19}ALP23	DLPC	0.70	133	30	0.9	0.65	158	44	1.6
	DMPC	0.71	138	15	1.2	0.66	143	59	1.4
	DOPC	0.68	142	4	1.0	0.61	160	42	0.5
GW^{3,21}ALP23	DLPC	0.50	11	10	1.3	0.50	162	41	3.5
	DMPC								
	DOPC								

[a]Entries left blank were not fitted. The angles ρ_1 and ρ_2 are defined in Figure S4 of the Supporting Information; see also ref 30. [b]S_{zz} is a dimensionless entity; ρ angles are in degrees, and rmsd is in kilohertz.

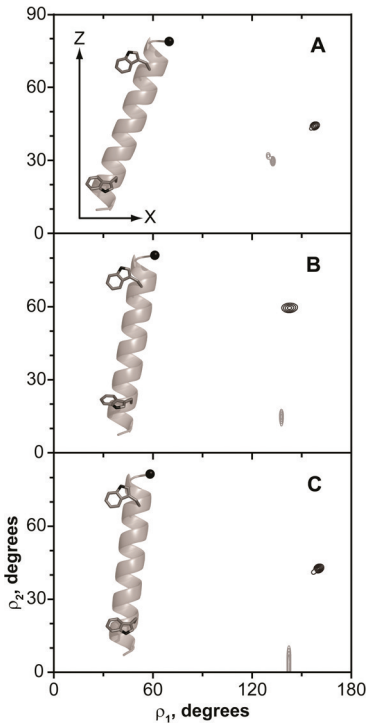

Figure 9. rmsd contour plots of the N-terminal (black) and C-terminal (gray) tryptophans of GW^{5,19}ALP23 as a function of indole ring orientation: (A) DLPC, (B) DMPC, and (C) DOPC. Contour levels are plotted every 1 kHz, with the outer contour corresponding to 5 kHz. Insets show one possible orientation of Trp side chains.

For GW^{3,21}ALP23, fits for both tryptophans were possible only in DLPC. Broad overlapped peaks for W3 in DMPC and DOPC make it hard to extract or assign $\Delta\nu_q$ values. Likewise, uncertainties in peak positions and observation of fewer than four resonances complicate the analysis also for W21. While combinations of plausible S_{zz}, ρ_1, and ρ_2 values that are similar to those of the N- or C-terminal Trp residues in other peptides can be obtained, it is not possible to exclude with confidence alternative assignments and consequently alternative ring orientations.

DISCUSSION

We have investigated the responses of model peptides having identical amino acid compositions and similar sequences, but different spacing between a pair of Trp residues that flank a central (Leu-Ala)$_n$ core helix, to lipid bilayer environments of differing lipid thickness. (We note in passing that when only two Trp residues are present in the sequence, the relatively polar Gly residues at positions 2 and 22 are of practical significance for the ease of synthesis, purification, and handling of the GWALP23 family peptides.) All of the peptides were able to incorporate into the DLPC, DMPC, and DOPC bilayer membranes. In every lipid tested, furthermore, each peptide retained a well-defined tilt angle, even in the potentially problematic case of a short spacing of the Trp residues, where tilting in a thicker lipid such as DOPC would be expected to drag Trp7 and Trp17 away from the interface in the direction of the bilayer center. A similar result has been observed in umbrella sampling simulations of WALP peptides and was explained in terms of a favorable entropy contribution arising from precession of the peptide about the lipid bilayer normal.[45,52]

Trp residues show a preference for the lipid−water interface in membrane proteins of known structure. A stabilization energy of ∼2 kcal/mol has been estimated per interfacial Trp residue in the *E. coli* OmpA protein.[15] In a "five-slab" membrane model, both Trp and Tyr partition to an 8 Å slab corresponding to the lipid headgroup region.[53] In 29 integral membrane proteins, the Trp and Tyr residues show saddlelike distributions with respect to the bilayer center, defining aromatic "belts" that are ∼10 Å wide and whose midpoints are separated by some 20−30 Å.[6] In comparison, because the helical repeat is 1.5 Å in length, the Trp residue separation in our peptides encompasses a similar range, from ∼15 Å in GW^{7,17}ALP23 to ∼27 Å in GW^{3,21}ALP23. From the low end to the high end of the range of aromatic residue separation, our results indicate notable differences in peptide properties.

Whole-Peptide Orientations and Dynamics. The analysis of GW^{3,21}ALP23 behavior in lipid bilayers suggests that the longer (Leu-Ala)$_{8.5}$ stretch undergoes more extensive whole-body motion relative to its shorter (Leu-Ala)$_{6.5}$ counterpart in GW^{5,19}ALP23 (Table 3). To gain additional insights into the nature of such motion, we have performed an analysis of explicit dynamics for both peptides in DLPC, using the ^{2}H NMR data. The semistatic analysis (Table 3) has suggested that the tilt angles of the two peptides are similar in DLPC, yet the S_{zz} values vary. To facilitate direct comparison, quadrupolar splittings from the identical alanine positions (7, 9, 11, 13, 15, and 17) were fitted for the two systems. The overall shapes of the tilt and rotation distributions (σ_τ and σ_ρ, respectively) are

similar for the $W^{3,21}$ and $W^{5,19}$ peptides in DLPC, with only moderate oscillations around the average values. The solution area for $GW^{5,19}$ALP23 is nevertheless more compact and shifted toward the lower σ_τ range (Figure 10). The somewhat higher σ_τ range for $GW^{3,21}$ALP23 is consistent with the correspondingly lower value of S_{zz} from the semistatic analysis (Table 3). The variations around the average ρ angle are close and fairly small for both the $W^{3,21}$ and $W^{5,19}$ peptides, indicating that neither peptide (each with only a single Trp residue near each terminus) undergoes extensive reorientation around the helix axis (in contrast to the extensive reorientation that is observed for WALP peptides when two Trp residues are present at each terminus). Furthermore, we note the close correspondence between the sets of average orientations of $GW^{x,y}$ALP23 peptides that are deduced from the semistatic (variable order parameter) and explicit (Gaussian distributions of τ and ρ) treatments of the whole-body dynamics. Both methods should be used with caution, as the semistatic approach will tend to overly simplify the dynamics, while the Gaussian approach introduces additional variable(s) into the analysis procedure, leading to a requirement for additional data points. The requirement can sometimes be met by combining the ^{2}H methyl quadrupolar splittings with ^{15}N-derived restraints[39,54] or, in selected cases, with backbone deuteron signals.[44] It is further of note that a more extensive treatment of $GW^{5,19}$ALP23 in DLPC, using combined ^{2}H and ^{15}N data with Gaussian dynamics, has led to the same tilt angle determined via semistatic analysis.[17]

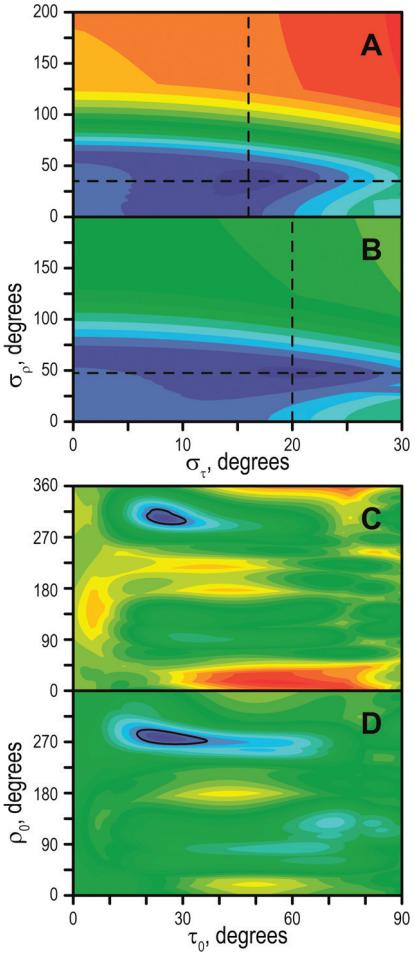

Figure 10. Explicit dynamics analysis of $GW^{5,19}$ALP23 (A and C) and $GW^{3,21}$ALP23 in DLPC (B and D), showing the standard deviations of Gaussian distributions (A and B) and their centers (C and D). Six alanine residues were used for the analysis (see the text). Dashed lines in panels A and B indicate the best fit σ_τ and σ_ρ, which were used for generating the plots in panels C and D, respectively. The color scale is identical between panels A and B (0 to 17 kHz, blue to red) and between panels C and D (0 to 22 kHz, blue to red). Color increments are 1 kHz; the solid lines in panels C and D are drawn at the 3 kHz level. Best fits (τ_0, σ_τ, ρ_0, and σ_ρ) are 25, 16, 303, and 36, respectively, for $GW^{5,19}$ALP23 and 25, 20, 278, and 48, respectively, for $GW^{3,21}$ALP23.

Earlier, we established that among different anchoring residues at the bilayer−water interface, tryptophans are major determinants of the transmembrane peptide orientation.[17] The design of $GW^{x,y}$ALP23 offers a way to investigate further details, because of the similar projections of the N- and C-terminal Trp residues from one side of the helical wheel. Additionally, the radial positions of the two Trp residues in $GW^{7,17}$ALP23 resemble closely those in $GW^{3,21}$ALP23, while the Trp residues in $GW^{5,19}$ALP23 project from a different face of the helix (Figure 1). Indeed, we find that $GW^{7,17}$ALP23 and $GW^{5,19}$ALP23 have nearly opposite ρ angles (Table 3), thus matching the change in the Trp radial positions, with each peptide tilting approximately in the direction of the tryptophans. Because of the similar projections of the two tryptophans, it is not yet possible to say whether either the N- or the C-terminal Trp may have a dominant role in determining the helix orientation in a lipid bilayer, although the advantageous design of GWALP23 will allow future testing of this feature. $GW^{3,21}$ALP23, on the other hand, does not seem to follow the same trend, perhaps because of the proximity of W3 and W21 to the peptide termini. Indeed, the fraying of the termini could impact the net radial projection of one or both Trp residues and thereby alter the preferred orientation of the backbone helix.

Minimum and Maximum Helix Tilt Angles in Lipid Bilayers. Examination of the $GW^{x,y}$ALP23 tilt angles reveals some correlation, but not a strictly linear trend between the Trp separation and the tilt magnitude (Table 3). This is particularly noticeable when the Trp spacing is small in a relatively thick bilayer, and vice versa. Thus, a minimum tilt angle of ~4° is observed for $GW^{7,17}$ALP23 in DOPC and DMPC, with only a slight increase in DLPC. On the other end of the scale are the values for $GW^{5,19}$ALP23 and $GW^{3,21}$ALP23 in DLPC, both tilting by approximately 20°. We note that the tilt angle of a single-span transmembrane peptide can be as much as 30°, when a charged residue is present within the core helix,[44] and possibly larger in helical bundles, where protein−protein interactions become vital. On the other hand, in cases such as $GW^{x,y}$ALP23 where the peptide tilt is governed largely by the lipid interactions of aromatic anchoring residues, it seems that minimum and maximum values of the tilt magnitude are observed.

We note moreover that the acyl chain unsaturation in DOPC will influence the lipid lateral pressure profile[16] at the same time that the longer acyl chains increase the DOPC bilayer hydrophobic thickness.[55] Indeed, both bilayer thickness and lateral pressure appear to be important for the changes in protein shape that accompany the gating of the MscL mechanosensitive channel.[56] Nevertheless, the rather flat behavior for the tilt of, for example, $GW^{7,17}$ALP23 among the three lipids tested here

dx.doi.org/10.1021/bi2006459 | Biochemistry 2011, 50, 7522–7535

suggests that the impact of lateral pressure as well as bilayer thickness upon helix tilt may be dampened in specific cases, particularly for neutral peptides with only aromatic anchor residues. We note furthermore that the $\Delta\nu_q$ magnitudes, for GW^{5,19}ALP23 in DMPC, show little variation between 1:40 and 1:200 peptide:lipid ratios (Figure S9 of the Supporting Information). In particular cases where the segment tilt depends only minimally on the packing density or the bilayer thickness, additional mechanisms, such as (partial) helix unwinding and/or reorientation of the side chain (indole ring) anchors, seem to help the peptides adapt to the lipid environment. These additional mechanisms also could be important for conformational changes that relate to membrane protein function.

Indole Ring Orientations. Deuterium labeling of the Trp residues allowed for definition of the orientations of the indole ring moieties with respect to the membrane normal in several cases (Table 6). Both the N- and C-terminal Trp residues are tightly clustered, albeit in different regions of conformational space. To visualize the indole ring orientations with respect to the tilted peptides, the ρ_1 and ρ_2 backbone-independent angles of 3-methylindole were converted to the Trp side chain χ_1 and χ_2 torsion angles, (Figure 11). Similar to the backbone-independent analysis, eight combinations of χ_1 and χ_2 led to the identical orientation of the indole ring with respect to the applied magnetic field. However, to serve as a membrane anchor, the Trp side chain should be positioned so that the $N_\varepsilon H$ bond vector points away from the bilayer center. This feature restricts the number of $\rho_{1,2}$ (or $\chi_{1,2}$) sets to four possible combinations (Figure S4 of the Supporting Information), as the $N_\varepsilon H$ bond vector should be directed along the positive Z-axis for the N-terminal Trp residues but along the negative Z-axis for the C-terminal Trp residues (see also refs 28, 30, 57, and 58). Additionally, in cases where ρ_2 is close to zero, the number of possible solutions is further reduced by half because of symmetry collapse (Figure S4 of the Supporting Information).

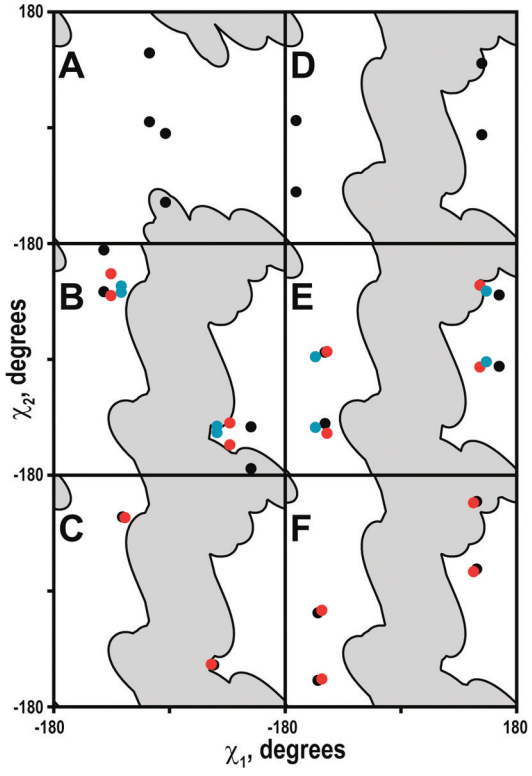

Figure 11. Tryptophan side chain torsion angles: (A) W3, (B) W5, (C) W7, (D) W21, (E) W19, and (F) W17. Gray regions indicate steric hindrance areas. Lipids are DLPC (black), DMPC (red), and DOPC (blue).

The possible side chain torsion angles of the N-terminal Trps fall into two major clusters (Figure 11A–C), with the indole carbon–carbon bridge (the common bond between the five- and six-membered rings) essentially either coaligned with the helix axis (negative χ_1, positive χ_2 cluster) or nearly perpendicular to it (positive χ_1, negative χ_2 cluster). Interestingly, both possible solutions are located close to the steric hindrance areas, suggesting that further changes in the Trp orientation are unfavorable, as they would include rearrangements of the backbone atoms. On the other hand, the orientations of the C-terminal Trp residues can be described by four possible combinations of χ_1 and χ_2 angles, in each case the bridge being virtually perpendicular to the helix axis (Figure 11D–F). While it appears that the C-terminal Trp residues are located farther from steric hindrance regions, it should be noted that these areas are approximate and are likely to change upon deviation from α-helical geometry, which was noted for some of the GW^{x,y}ALP23 peptides (see Results). While deuterium NMR alone does not allow us to distinguish among the possible solutions, the choices of side chain torsion angles could be further refined through distance measurements obtained by solution or magic angle spinning NMR.

The analysis of Trp side chain geometry has been previously reported for WALP peptides (having two sequential Trp residues in the proximity of the N- and C-termini) in DMPC and its ether analogue.[28] Certain similarities can be seen for the Trp residues at the N- or C-termini of WALP and GW^{x,y}ALP23 peptides. The dynamic behavior of the N-terminal Trps is closely similar between the two systems, the order parameters being approximately 0.7. In the case of the C-terminal Trp residues, two minima have been observed for WALP peptides, with S_{zz} values of 0.45 and 0.6. The results for the GW^{x,y}ALP23 peptides suggest that the minimum with the higher order parameter better reflects the state of the system. In terms of the average indole orientation with respect to the applied magnetic field, three of the Trp residues in WALP19 adopt ρ_1 and ρ_2 angles that resemble closely those found for corresponding Trp residues in GW^{x,y}ALP23 (Figure S12 of the Supporting Information). Interestingly, only Trp18 in WALP19 seems not to fall within the cluster defined by the other C-terminal Trp residues that have been examined in WALP and GWALP peptides, mainly because of a difference in the ρ_1 angle.

GW^{3,21}ALP23 is similar to a WALP sequence in terms of the proximity of Trp to the helix termini. It is notable that the Trp steric hindrance areas are smaller for this peptide. This result is particularly manifest for W3 because of the direction of the C_α–C_β bond vector pointing toward the N-terminus, thereby effectively shifting all side chains marginally closer to the N-terminus. Interestingly, for GW^{3,21}ALP23, it was possible to assign the indole quadrupolar splittings only in DLPC, as the resonances were broader and less well-defined in other lipids, suggesting more complex dynamics. The steric hindrance patterns for WALP peptides are expected to be complicated because of the locations of two bulky Trp side chains next to each other, meaning that the orientation of each indole moiety could be influenced by the adjacent tryptophan. If such

dx.doi.org/10.1021/bi2006459 | Biochemistry 2011, 50, 7522–7535

indole−indole restrictions are nevertheless ignored, the Trp residues at the C-terminus are expected to have less conformational freedom, as a χ_1 angle near 0° would lead to the severe clashes with the backbone of residues $i-3$ and $i-4$. The steric hindrance area for the C-terminal Trp residues, therefore, changes only marginally as Trp approaches the peptide terminus (Figure 11D−F).

Overall, the variations in the indole ring orientations were smaller than the variations in helix tilt angles for the different peptide−lipid combinations. The results imply that the Trp side chain undergoes changes in the χ_1 and χ_2 torsion angles to compensate in part for changes in the helix tilt. By this mechanism, a particular Trp will be able to maintain a similar indole orientation and a similar lipid interaction, which presumably provides effective anchoring, as the peptide changes its tilt. A single Trp side chain near the N-terminus samples a larger range of conformational space in response to a change in the lipid thickness, although the primary adjustment would seem to involve only one of the χ angles (Figure 11). The response of a C-terminal Trp appears to be less systematic and to involve both χ angles to similar extents.

CONCLUDING PERSPECTIVE

GWALP23 peptide isomers having different core helix lengths of 10, 14, and 18 residues between a single pair of anchoring Trp residues display systematic responses to lipid bilayer membranes of differing thickness and extent of acyl chain unsaturation. The responses include adjustments to the peptide tilt between apparent limits of ∼5° and just over 20° with respect to the bilayer normal. Further adjustments to the helix tilt seem to be dampened by potentially compensating adjustments involving the indole ring orientations and the whole-body dynamics, along with variable fraying of the ends of the helix. The responses of the peptides to differing lipid bilayer environments therefore involve combinations of multiple factors. Similar principles are likely to govern the behavior and function of the transmembrane domains of single-span membrane proteins.

ASSOCIATED CONTENT

Supporting Information

Proton NMR spectra of Fmoc-Trp-d_2, definition of ρ angles, physical data for GW^{x,y}ALP23 peptides (HPLC, mass spectra), and deuterium NMR spectra of peptides in DLPC, DMPC, and DOPC. This material is available free of charge via the Internet at http://pubs.acs.org.

AUTHOR INFORMATION

Corresponding Author

*Current address: 312 Church St. SE, Hasselmo Hall, 5-250A, University of Minnesota, Minneapolis, MN 55455. Telephone: (612) 625-0786. Fax: (612) 625-2163. E-mail: vvostri@gmail.com.

Funding

This work was supported in part by National Science Foundation Grant MCB-0841227 and the Arkansas Biosciences Institute.

ACKNOWLEDGMENTS

We thank James Hinton and Denise Greathouse for helpful discussions. The peptide and NMR facilities were supported by National Institutes of Health Grants RR31154 and RR16460.

ABBREVIATIONS

CD, circular dichroism; DLPC, 1,2-dilauroyl-*sn*-glycero-3-phosphocholine; DMPC, 1,2-dimyristoyl-*sn*-glycero-3-phosphocholine; DOPC, 1,2-dioleoyl-*sn*-glycero-3-phosphocholine; Fmoc, fluorenylmethoxycarbonyl; GALA, geometric analysis of labeled alanines; rmsd, root-mean-square deviation; TFA, trifluoroacetic acid.

REFERENCES

(1) Park, S. H., De Angelis, A. A., Nevzorov, A. A., Wu, C. H., and Opella, S. J. (2006) Three-dimensional structure of the transmembrane domain of Vpu from HIV-1 in aligned phospholipid bicelles. *Biophys. J. 91*, 3032−3042.

(2) Kandasamy, S. K., Lee, D. K., Nanga, R. P., Xu, J., Santos, J. S., Larson, R. G., and Ramamoorthy, A. (2009) Solid-state NMR and molecular dynamics simulations reveal the oligomeric ion-channels of TM2-GABA$_A$ stabilized by intermolecular hydrogen bonding. *Biochim. Biophys. Acta 1788*, 686−695.

(3) Schick, S., Chen, L., Li, E., Lin, J., Koper, I., and Hristova, K. (2010) Assembly of the M2 tetramer is strongly modulated by lipid chain length. *Biophys. J. 99*, 1810−1817.

(4) Brown, M. F. (1994) Modulation of rhodopsin function by properties of the membrane bilayer. *Chem. Phys. Lipids 73*, 159−180.

(5) Landolt-Marticorena, C., Williams, K. A., Deber, C. M., and Reithmeier, R. A. (1993) Non-random distribution of amino acids in the transmembrane segments of human type I single span membrane proteins. *J. Mol. Biol. 229*, 602−608.

(6) Ulmschneider, M. B., and Sansom, M. S. P. (2001) Amino acid distributions in integral membrane protein structures. *Biochim. Biophys. Acta 1512*, 1−14.

(7) de Planque, M. R., Kruijtzer, J. A., Liskamp, R. M., Marsh, D., Greathouse, D. V., Koeppe, R. E. II, de Kruijff, B., and Killian, J. A. (1999) Different membrane anchoring positions of tryptophan and lysine in synthetic transmembrane α-helical peptides. *J. Biol. Chem. 274*, 20839−20846.

(8) Davis, J. H., Clare, D. M., Hodges, R. S., and Bloom, M. (1983) Interaction of a synthetic amphiphilic polypeptide and lipids in a bilayer structure. *Biochemistry 22*, 5298−5305.

(9) Killian, J. A., Salemink, I., de Planque, M. R., Lindblom, G., Koeppe, R. E. II, and Greathouse, D. V. (1996) Induction of nonbilayer structures in diacylphosphatidylcholine model membranes by transmembrane α-helical peptides: Importance of hydrophobic mismatch and proposed role of tryptophans. *Biochemistry 35*, 1037−1045.

(10) Harzer, U., and Bechinger, B. (2000) Alignment of lysine-anchored membrane peptides under conditions of hydrophobic mismatch: A CD, ^{15}N and ^{31}P solid-state NMR spectroscopy investigation. *Biochemistry 39*, 13106−13114.

(11) Krishnakumar, S. S., and London, E. (2007) Effect of sequence hydrophobicity and bilayer width upon the minimum length required for the formation of transmembrane helices in membranes. *J. Mol. Biol. 374*, 671−687.

(12) van der Wel, P. C., Strandberg, E., Killian, J. A., and Koeppe, R. E. II (2002) Geometry and intrinsic tilt of a tryptophan-anchored transmembrane α-helix determined by ^{2}H NMR. *Biophys. J. 83*, 1479−1488.

(13) Strandberg, E., Ozdirekcan, S., Rijkers, D. T., van der Wel, P. C., Koeppe, R. E. II, Liskamp, R. M., and Killian, J. A. (2004) Tilt angles of transmembrane model peptides in oriented and non-oriented lipid bilayers as determined by ^{2}H solid-state NMR. *Biophys. J. 86*, 3709−3721.

(14) de Planque, M. R., Bonev, B. B., Demmers, J. A., Greathouse, D. V., Koeppe, R. E. II, Separovic, F., Watts, A., and Killian, J. A. (2003) Interfacial anchor properties of tryptophan residues in transmembrane

peptides can dominate over hydrophobic matching effects in peptide-lipid interactions. *Biochemistry 42*, 5341−5348.

(15) Hong, H., Park, S., Jimenez, R. H., Rinehart, D., and Tamm, L. K. (2007) Role of aromatic side chains in the folding and thermodynamic stability of integral membrane proteins. *J. Am. Chem. Soc. 129*, 8320−8327.

(16) Binder, H., and Gawrisch, K. (2001) Effect of unsaturated lipid chains on dimensions, molecular order and hydration of membranes. *J. Phys. Chem. B 105*, 12378−12390.

(17) Vostrikov, V. V., Daily, A. E., Greathouse, D. V., and Koeppe, R. E. II (2010) Charged or aromatic anchor residue dependence of transmembrane peptide tilt. *J. Biol. Chem. 285*, 31723−31730.

(18) Petrache, H. I., Zuckerman, D. M., Sachs, J. N., Killian, J. A., Koeppe, R. E. II, and Woolf, T. B. (2002) Hydrophobic matching mechanism investigated by molecular dynamics simulations. *Langmuir 18*, 1340−1351.

(19) Liu, J., Wang, D., Zheng, Q., Lu, M., and Arora, P. S. (2008) Atomic structure of a short α-helix stabilized by a main chain hydrogen-bond surrogate. *J. Am. Chem. Soc. 130*, 4334−4337.

(20) Froyd-Rankenberg, J. M., Greathouse, D. V., and Koeppe, R. E. II (2009) Half-anchored WALP peptides: Effect of anchor position on peptide orientation. *Biophys. J. 96*, 455a−456a.

(21) Vostrikov, V. V., Grant, C. V., Daily, A. E., Opella, S. J., and Koeppe, R. E. II (2008) Comparison of "Polarization Inversion with Spin Exchange at Magic Angle" and "Geometric Analysis of Labeled Alanines" methods for transmembrane helix alignment. *J. Am. Chem. Soc. 130*, 12584−12585.

(22) Strandberg, E., Esteban-Martin, S., Salgado, J., and Ulrich, A. S. (2009) Orientation and dynamics of peptides in membranes calculated from ^{2}H-NMR data. *Biophys. J. 96*, 3223−3232.

(23) Holt, A., Rougier, L., Reat, V., Jolibois, F., Saurel, O., Czaplicki, J., Killian, J. A., and Milon, A. (2010) Order parameters of a transmembrane helix in a fluid bilayer: Case study of a WALP peptide. *Biophys. J. 98*, 1864−1872.

(24) Ozdirekcan, S., Rijkers, D. T., Liskamp, R. M., and Killian, J. A. (2005) Influence of flanking residues on tilt and rotation angles of transmembrane peptides in lipid bilayers. A solid-state ^{2}H NMR study. *Biochemistry 44*, 1004−1012.

(25) Vostrikov, V. V., Hall, B. A., Greathouse, D. V., Koeppe, R. E. II, and Sansom, M. S. P. (2010) Changes in transmembrane helix alignment by arginine residues revealed by solid-state NMR experiments and coarse-grained MD simulations. *J. Am. Chem. Soc. 132*, 5803−5811.

(26) O'Connell, A. M., Koeppe, R. E. II, and Andersen, O. S. (1990) Kinetics of gramicidin channel formation in lipid bilayers: Transmembrane monomer association. *Science 250*, 1256−1259.

(27) Yau, W. M., Wimley, W. C., Gawrisch, K., and White, S. H. (1998) The preference of tryptophan for membrane interfaces. *Biochemistry 37*, 14713−14718.

(28) van der Wel, P. C., Reed, N. D., Greathouse, D. V., and Koeppe, R. E. II (2007) Orientation and motion of tryptophan interfacial anchors in membrane-spanning peptides. *Biochemistry 46*, 7514−7524.

(29) ten Kortenaar, P. B. W., Van Dijk, B. G., Peeters, J. M., Raaben, B. J., Adams, P. J. H. M., and Tesser, G. I. (1986) Rapid and efficient method for the preparation of Fmoc-amino acids starting from 9-fluorenylmethanol. *Int. J. Pept. Protein Res. 27*, 398−400.

(30) Koeppe, R. E. II, Sun, H., van der Wel, P. C., Scherer, E. M., Pulay, P., and Greathouse, D. V. (2003) Combined experimental/theoretical refinement of indole ring geometry using deuterium magnetic resonance and ab initio calculations. *J. Am. Chem. Soc. 125*, 12268−12276.

(31) Greathouse, D. V., Koeppe, R. E. II, Providence, L. L., Shobana, S., and Andersen, O. S. (1999) Design and characterization of gramicidin channels. *Methods Enzymol. 294*, 525−550.

(32) Davis, J. H., Jeffrey, K. R., Bloom, M., Valic, M. I., and Higgs, T. P. (1976) Quadrupolar echo deuteron magnetic resonance spectroscopy in ordered hydrocarbon chains. *Chem. Phys. Lett. 42*, 390−394.

(33) Pulay, P., Scherer, E. M., van der Wel, P. C., and Koeppe, R. E. II (2005) Importance of tensor asymmetry for the analysis of ^{2}H NMR spectra from deuterated aromatic rings. *J. Am. Chem. Soc. 127*, 17488−17493.

(34) Sun, H., Greathouse, D. V., Andersen, O. S., and Koeppe, R. E. II (2008) The preference of tryptophan for membrane interfaces: Insights from N-methylation of tryptophans in gramicidin channels. *J. Biol. Chem. 283*, 22233−22243.

(35) Guex, N., and Peitsch, M. C. (1997) SWISS-MODEL and the Swiss-PdbViewer: An environment for comparative protein modeling. *Electrophoresis 18*, 2714−2723.

(36) Monera, O. D., Sereda, T. J., Zhou, N. E., Kay, C. M., and Hodges, R. S. (1995) Relationship of sidechain hydrophobicity and α-helical propensity on the stability of the single-stranded amphipathic α-helix. *J. Pept. Sci. 1*, 319−329.

(37) White, S. H., and von Heijne, G. (2008) How translocons select transmembrane helices. *Annu. Rev. Biophys. 37*, 23−42.

(38) Granseth, E., von Heijne, G., and Elofsson, A. (2005) A study of the membrane-water interface region of membrane proteins. *J. Mol. Biol. 346*, 377−385.

(39) Aisenbrey, C., and Bechinger, B. (2004) Tilt and rotational pitch angle of membrane-inserted polypeptides from combined ^{15}N and ^{2}H solid-state NMR spectroscopy. *Biochemistry 43*, 10502−10512.

(40) Hessa, T., Kim, H., Bihlmaier, K., Lundin, C., Boekel, J., Andersson, H., Nilsson, I., White, S. H., and von Heijne, G. (2005) Recognition of transmembrane helices by the endoplasmic reticulum translocon. *Nature 433*, 377−381.

(41) Bechinger, B., Skladnev, D. A., Ogrel, A., Li, X., Rogozhkina, E. V., Ovchinnikova, T. V., O'Neil, J. D., and Raap, J. (2001) ^{15}N and ^{31}P solid-state NMR investigations on the orientation of zervamicin II and alamethicin in phosphatidylcholine membranes. *Biochemistry 40*, 9428−9437.

(42) Salnikov, E. S., Friedrich, H., Li, X., Bertani, P., Reissmann, S., Hertweck, C., O'Neil, J. D., Raap, J., and Bechinger, B. (2009) Structure and alignment of the membrane-associated peptaibols ampullosporin A and alamethicin by oriented ^{15}N and ^{31}P solid-state NMR spectroscopy. *Biophys. J. 96*, 86−100.

(43) Salnikov, E. S., and Bechinger, B. (2011) Lipid-controlled peptide topology and interactions in bilayers: Structural insights into the synergistic enhancement of the antimicrobial activities of PGLa and magainin 2. *Biophys. J. 100*, 1473−1480.

(44) Vostrikov, V. V. (2011) Protein-lipid interactions: Influence of anchoring groups and buried arginine on the properties of membrane-spanning peptides, Ph.D. Thesis, University of Arkansas, Fayetteville, AR.

(45) Lee, J., and Im, W. (2008) Transmembrane helix tilting: Insights from calculating the potential of mean force. *Phys. Rev. Lett. 100*, 018103.

(46) Ozdirekcan, S., Etchebest, C., Killian, J. A., and Fuchs, P. F. J. (2007) On the orientation of a designed transmembrane peptide: Toward the right tilt angle? *J. Am. Chem. Soc. 129*, 15174−15181.

(47) Esteban-Martin, S., and Salgado, J. (2007) The dynamic orientation of membrane-bound peptides: Bridging simulations and experiments. *Biophys. J. 93*, 4278−4288.

(48) MacCallum, J. L., Bennett, W. F., and Tieleman, D. P. (2008) Distribution of amino acids in a lipid bilayer from computer simulations. *Biophys. J. 94*, 3393−3404.

(49) Hessa, T., Meindl-Beinker, N. M., Bernsel, A., Kim, H., Sato, Y., Lerch-Bader, M., Nilsson, I., White, S. H., and von Heijne, G. (2007) Molecular code for transmembrane-helix recognition by the Sec61 translocon. *Nature 450*, 1026−1030.

(50) Wiener, M. C., and White, S. H. (1992) Structure of a fluid dioleoylphosphatidylcholine bilayer determined by joint refinement of

X-ray and neutron diffraction data. III. Complete structure. *Biophys. J. 61*, 434−447.

(51) Lakowicz, J. R. (2006) *Principles of Fluorescence Spectroscopy*, 3rd ed., Springer, Berlin.

(52) Kim, T., and Im, W. (2010) Revisiting hydrophobic mismatch with free energy simulation studies of transmembrane helix tilt and rotation. *Biophys. J. 99*, 175−183.

(53) Sengupta, D., Smith, J. C., and Ullmann, G. M. (2008) Partitioning of amino-acid analogues in a five-slab membrane model. *Biochim. Biophys. Acta 1778*, 2234−2243.

(54) Bechinger, B., Resende, J. M., and Aisenbrey, C. (2011) The structural and topological analysis of membrane-associated polypeptides by oriented solid-state NMR spectroscopy: Established concepts and novel developments. *Biophys. Chem. 153*, 115−125.

(55) Marsh, D. (2008) Energetics of hydrophobic matching in lipid-protein interactions. *Biophys. J. 94*, 3996−4013.

(56) Samuli Ollila, O. H., Louhivuori, M., Marrink, S. J., and Vattulainen, I. (2011) Protein shape change has a major effect on the gating energy of a mechanosensitive channel. *Biophys. J. 100*, 1651−1659.

(57) Koeppe, R. E. II, Killian, J. A., and Greathouse, D. V. (1994) Orientations of the tryptophan 9 and 11 side chains of the gramicidin channel based on deuterium nuclear magnetic resonance spectroscopy. *Biophys. J. 66*, 14−24.

(58) Hu, W., Lazo, N. D., and Cross, T. A. (1995) Tryptophan dynamics and structural refinement in a lipid bilayer environment: Solid state NMR of the gramicidin channel. *Biochemistry 34*, 14138−14146.

(59) de Planque, M. R., and Killian, J. A. (2003) Protein-lipid interactions studied with designed transmembrane peptides: Role of hydrophobic matching and interfacial anchoring. *Mol. Membr. Biol. 20*, 271−284.